Modulational instability of ion acoustic waves in a multi-species collisionless magnetized plasma consisting of nonthermal and isothermal electrons

Sandip Dalui, Anup Bandyopadhyay, and K. P. Das

Citation: Physics of Plasmas **24**, 102310 (2017); doi: 10.1063/1.4991806
View online: http://dx.doi.org/10.1063/1.4991806
View Table of Contents: http://aip.scitation.org/toc/php/24/10
Published by the American Institute of Physics

PHYSICS OF PLASMAS **24**, 102310 (2017)

Modulational instability of ion acoustic waves in a multi-species collisionless magnetized plasma consisting of nonthermal and isothermal electrons

Sandip Dalui,[1] Anup Bandyopadhyay,[1,a)] and K. P. Das[2]
[1]*Department of Mathematics, Jadavpur University, Kolkata 700032, India*
[2]*Department of Applied Mathematics, University of Calcutta, Kolkata 700009, India*

(Received 23 June 2017; accepted 7 September 2017; published online 27 September 2017)

This paper is an extension of the recent work of Dalui *et al.* [Phys. Plasmas **24**, 042305 (2017)] on modulational instability of ion acoustic waves in a multi-species collisionless plasma by considering the effect of uniform (space independent) and static (time independent) magnetic field directed along a fixed direction. A three dimensional nonlinear Schrödinger equation is derived to study the modulational instability of ion acoustic waves in a multi-species collisionless magnetized plasma consisting of warm adiabatic ions, nonthermal hot electrons, due to Cairns *et al.* [Geophys. Res. Lett. **22**, 2709 (1995)], which generates the fast energetic electrons and Maxwell-Boltzmann distributed isothermal electrons. The modulational instability of ion acoustic waves propagating along the direction of the magnetic field has been investigated theoretically. The instability condition and the maximum growth rate of instability have been derived analytically. It is found that the maximum growth rate of instability decreases with increasing values of the magnetic field intensity whereas the maximum growth rate of instability increases with increasing $\cos\delta$, where δ is directly related to the modulational obliqueness θ by the relation $\theta + \delta = \frac{\pi}{2}$, i.e., δ is the angle between the direction of the modulated wave with the static uniform magnetic field. *Published by AIP Publishing.* https://doi.org/10.1063/1.4991806

I. INTRODUCTION

Plasmas with different species of electrons at different temperatures have been observed by various spacecraft missions, viz., FAST at the auroral region,[1–5] Viking Satellite,[6,7] S3-3 Satellite,[8] GEOTAIL,[9] and POLAR[5,10,11] missions in the Earth's magnetosphere. Studies of two–electron–temperature plasma by these satellite observations of moving localized potential variation regions not necessarily indicate that the distribution functions of both the electron species are isothermal. Specifically, the observations of electric field structures by the FAST[1–5] satellite, Viking Satellite,[6,7] and Freja Satellite[12] in the auroral zone indicate the existence of energetic electrons along with isothermal electrons. Thus, there may exist two different species of electrons at different temperatures in the auroral zone of the magnetosphere and ionosphere of the Earth. Among these two species of electrons, one species of electrons follows Maxwell-Boltzmann distribution and the other species of fast energetic electrons can be taken as the nonthermal velocity distribution of Cairns *et al.*[13] Although different non-Maxwellian distributions have been modeled in phase space to describe the behaviour of the energetic particles, the electrostatic wave structures observed by the Freja Satellite[12] can be best described by considering Cairns[13] distributed nonthermal electrons and using this nonthermal distribution of electrons, Cairns *et al.*[14] investigated ion acoustic (IA) solitary waves in a collisionless magnetized electron ion plasma. Later Mamun and Cairns[15] investigated the stability of solitary waves in a magnetized nonthermal plasma. Bandyopadhyay and Das[16] investigated the effect of Landau damping on IA solitary waves in a magnetized nonthermal plasma. Islam *et al.*[17] considered a collisionless magnetized electron–ion plasma system consisting of warm adiabatic ions and a superposition of two distinct populations of electrons at different temperatures, a cooler one with a Boltzmann distribution and a hotter one with a nonthermal Cairns distribution to investigate the small amplitude IA solitary waves. Recently, Rufai *et al.*[18] investigated the arbitrary amplitude solitary structures in a collisionless magnetized electron ion plasma system consisting of cold ions, nonthermal hot electrons, and Boltzmann distributed isothermal electrons giving a special emphasis on IA supersolitons. Several authors[19–28] investigated the nonlinear properties of arbitrary amplitude IA solitary waves in an unmagnetized plasma consisting of two different populations of electron species (both the electron species follow Boltzmann-Maxwellian distribution) at different temperatures.

Recently, Dalui *et al.*[29] have investigated the modulational instability (MI) of IA waves in a collisionless unmagnetized plasma consisting of warm adiabatic ions and a superposition of two distinct populations of electrons, one due to Cairns *et al.*,[13] which generates the fast energetic electrons, and the other the well known Maxwell-Boltzmann distributed electrons. Using Reductive Perturbation Method (RPM),[30,31] they have derived a one dimensional nonlinear Schrödinger equation (NLSE). The instability condition and the maximum growth rate of instability have been derived. In the present paper, we have extended the earlier work of Dalui *et al.*[29] by considering the effect of uniform static magnetic field directed along a fixed direction.

The MI of IA envelop solitary waves in multi-species unmagnetized two temperature electron plasma have been

[a)]Electronic mail: abandyopadhyay1965@gmail.com

studied by several authors.[32–37] Kako[38] investigated the MI of IA waves in a magnetized plasma. Murtaza and Salahuddin[39] investigated the MI of IA waves in a collisionless magnetized plasma consisting of cold ions and isothermal electrons. Misra and Roy Chowdhury[40] investigated the MI of IA waves in a collisional magnetized plasma consisting of adiabatic warm ions and nonthermal electrons. Shukla and Misra[41] investigated the amplitude modulation of low-frequency, long-wavelength electrostatic drift wave packets in a nonuniform magnetoplasma with the effects of equilibrium density, electron temperature, and magnetic field inhomogeneities by deriving a NLSE. They reported that the modulated drift wave packet can propagate in the form of bright and dark envelope solitons or as a drift rogue wave. Misra[42] considered the similar problem in quantum magnetoplasma. Beside these, several authors[43–47] investigated the MI of IA waves in different magnetized plasma systems.

In this paper, we have investigated the nonlinear evolution of modulated IA waves in a fully ionized collisionless plasma consisting of warm adiabatic ions and two species of electrons at different temperatures, a cooler one with a Boltzmann distribution and a hotter one with a nonthermal Cairns distribution, immersed in a uniform static magnetic field directed along a fixed direction. The MI of IA waves propagating along the direction of the uniform static magnetic field has been investigated theoretically. A three dimensional nonlinear Schrödinger equation is derived to investigate the MI of the obliquely modulated IA waves. The instability condition and the maximum growth rate of instability have been derived analytically.

II. BASIC EQUATIONS

We consider a fully ionized collisionless plasma consisting of warm adiabatic ions and two species of electrons at different temperatures, a cooler one with a Boltzmann distribution and a hotter one with a nonthermal Cairns distribution immersed in a uniform static magnetic field ($\mathbf{B} = B_0\hat{\mathbf{z}}$) directed along z-axis. The basic equations of the present plasma system are given by

$$\frac{\partial n}{\partial t} + \nabla\cdot(n\mathbf{u}) = 0, \tag{1}$$

$$\frac{\partial \mathbf{u}}{\partial t} + (\mathbf{u}\cdot\nabla)\mathbf{u} = -\nabla\phi + \omega_c(\mathbf{u}\times\hat{\mathbf{z}}) - \frac{\sigma}{n}\nabla p, \tag{2}$$

$$\nabla^2\phi = n_{ce} + n_{se} - n, \tag{3}$$

$$p = n^{\gamma}, \tag{4}$$

where $\nabla \equiv \left(\frac{\partial}{\partial x}, \frac{\partial}{\partial y}, \frac{\partial}{\partial z}\right)$.

Here, n, n_{ce}, n_{se}, ω_c, $\mathbf{u} = (u, v, w)$, p, ϕ, (x, y, z), and t are the ion number density, the nonthermal electron number density, the isothermal electron number density, the ion cyclotron frequency, the ion fluid velocity, the ion pressure, the electrostatic potential, the spatial variables, and time, respectively, and these quantities have been normalized by n_0, n_0, n_0, $\omega_{pi}\left(=\sqrt{4\pi n_0 e^2/m}\right)$, $c_s\left(=\sqrt{K_B T_{ef}/m}\right)$, $n_0 K_B T_i$, $K_B T_{ef}/e$, $\lambda_{Df}\left(=\sqrt{K_B T_{ef}/4\pi n_0 e^2}\right)$, and ω_{pi}^{-1}, where $\sigma = T_i/T_{ef}$ and $\gamma\left(=\frac{5}{3}\right)$ is the ratio of two specific heats. Again, K_B is the Boltzmann constant, n_0 is the unperturbed ion number density, m is the mass of an ion, $-e$ is the charge of an electron, T_i is the average ion temperature, and T_{ef} is given by the following equation:

$$\frac{n_{c0} + n_{s0}}{T_{ef}} = \frac{n_{c0}}{T_{ce}} + \frac{n_{s0}}{T_{se}}, \tag{5}$$

where n_{c0}, n_{s0}, T_{ce}, and T_{se} are unperturbed nonthermal electron number density, unperturbed isothermal electron number density, average temperature of nonthermal electrons, and average temperature of isothermal electrons, respectively.

Based on the above-mentioned normalization of the independent and dependent variables, the normalized number density of Cairns[13] distributed nonthermal electrons and the normalized number density of isothermal electrons can be written as

$$n_{ce} = \bar{n}_{c0}(1 - \beta_e\sigma_c\phi + \beta_e\sigma_c^2\phi^2)\exp[\sigma_c\phi], \tag{6}$$

$$n_{se} = \bar{n}_{s0}\exp[\sigma_s\phi], \tag{7}$$

where $\beta_e = \frac{4\alpha_e}{1+3\alpha_e}$ with $\alpha_e \geq 0$, $\bar{n}_{c0} = \frac{n_{c0}}{n_0}$, $\bar{n}_{s0} = \frac{n_{s0}}{n_0}$, $\sigma_c = \frac{T_{ef}}{T_{ce}}$, $\sigma_s = \frac{T_{ef}}{T_{se}}$.

Here, β_e is the nonthermal parameter, and according to Verheest and Pillay,[48] the physically admissible bounds of β_e is given by $0 \leq \beta_e \leq \frac{4}{7} \approx 0.6$. Now, Eq. (5) and the charge neutrality condition ($n_{c0} + n_{s0} = n_0$) can be written as

$$\bar{n}_{c0}\sigma_c + \bar{n}_{s0}\sigma_s = 1, \quad \bar{n}_{c0} + \bar{n}_{s0} = 1. \tag{8}$$

Introducing the new parameters $\sigma_{sc} = \frac{T_{se}}{T_{ce}}$ and $n_{sc} = \frac{n_{s0}}{n_{c0}}$, the expressions of $\bar{n}_{c0}$, $\bar{n}_{s0}$, σ_c, and σ_s can be simplified as follows:

$$\bar{n}_{s0} = \frac{n_{sc}}{1+n_{sc}}, \quad \bar{n}_{c0} = \frac{1}{1+n_{sc}}, \tag{9}$$

$$\sigma_s = \frac{1+n_{sc}}{\sigma_{sc}+n_{sc}}, \quad \sigma_c = \sigma_{sc}\frac{1+n_{sc}}{\sigma_{sc}+n_{sc}}, \tag{10}$$

where we have used Eq. (8) to get Eqs. (9) and (10).

Expanding both n_{ce} and n_{se} as given by (6) and (7), respectively, using the charge neutrality condition and keeping the terms up to ϕ^3, we can write the Poisson equation (3) as

$$\nabla^2\phi = h_0 + h_1\phi + h_2\phi^2 + h_3\phi^3 - n, \tag{11}$$

where h_0, h_1, h_2, and h_3 are given by

$$h_0 = 1, \quad h_1 = (1 - \beta_e\bar{n}_{c0}\sigma_c), \tag{12}$$

$$h_2 = \frac{1}{2}\left[\bar{n}_{s0}\sigma_s^2 + \bar{n}_{c0}\sigma_c^2\right], \tag{13}$$

$$h_3 = \frac{1}{6}\left[\bar{n}_{s0}\sigma_s^3 + \bar{n}_{c0}(1+3\beta_e)\sigma_c^3\right]. \tag{14}$$

III. DERIVATION OF THE NLSE

In order to discuss the MI of IA waves propagating along z-axis in a collisionless magnetized plasma, we consider the linear dispersion relation of the IA wave propagating along

z-axis. Linearising Eqs. (1), (2), (4), and (11) with respect to the dependent variables, assuming space-time dependence of the dependent variables to be of the form $\exp[i(kz-\omega t)]$, the linear dispersion relation of the IA wave propagating along the direction of the magnetic field ($\mathbf{B}=B_0\hat{\mathbf{z}}$) can be written as

$$\frac{\omega}{k}=\sqrt{\sigma\gamma+\frac{1}{k^2+h_1}}. \qquad (15)$$

This equation shows that wave frequency ω can be expressed as a function of k and we can write $\omega=\omega(k)$.

To describe the nonlinear amplitude modulational of the IA wave (carrier wave) satisfying the dispersion relation (15) having central wave number k and wave frequency $\omega(=\omega(k))$, let us consider a disturbance which produces a perturbation ϵ in the wave number k. For this wave with wave number $k+\epsilon$, the wave frequency $\omega(k+\epsilon)$ can be expanded in Taylor series as

$$\omega(k+\epsilon)=\omega(k)+\epsilon\frac{\partial\omega}{\partial k}+\epsilon^2\left[\frac{1}{2}\frac{\partial^2\omega}{\partial k^2}\right]+O(\epsilon^3). \qquad (16)$$

Therefore, for the perturbation ϵ in the wave number k, the change in phase ($\delta\psi$) can be written as

$$\begin{aligned}\delta\psi&=[(k+\epsilon)z-\omega(k+\epsilon)t]-[kz-\omega(k)t]\\&=\epsilon\left[z-\frac{\partial\omega}{\partial k}t\right]+\left[-\frac{1}{2}\frac{\partial^2\omega}{\partial k^2}\right](\epsilon^2 t)+O(\epsilon^3).\end{aligned} \qquad (17)$$

Therefore, for the slow amplitude modulation of the plane wave perturbation of the carrier wave, Eq. (17) guides us to choose the stretched spatial variables[30,49,50] along the direction of the magnetic field as $\zeta=\epsilon\left(z-\frac{\partial\omega}{\partial k}t\right)$ and stretched time[30,49,50] as $\tau=\epsilon^2 t$. Therefore, in the coordinate frame moving with a velocity $\frac{\partial\omega}{\partial k}$, the time variation of the wave packets appears very slow. Although the IA wave is propagating along the direction of the magnetic field, due to the introduction of the magnetic field, the weak dependence of the spatial coordinates perpendicular to the direction of the uniform static magnetic field is taken into account because the inclusion of the magnetic field results in overall inhomogeneity in plasma. On the other hand, weak dependence of the spatial coordinates perpendicular to the direction of the uniform static magnetic field also help us to study the stability of modulated IA wave [i.e., when modulation on the wave amplitude (packet) takes place] with oblique modulation.

So, in order to study the MI of IA waves propagating along z-axis in a collisionless magnetized plasma, we have used the following stretchings of the spatial coordinates and time:

$$\xi=\epsilon x,\quad \eta=\epsilon y,\quad \zeta=\epsilon(z-V_g t),\quad \tau=\epsilon^2 t, \qquad (18)$$

where ϵ is a small parameter and V_g can be determined later by considering the compatibility condition and we will see that the value of V_g is exactly same as $\frac{\partial\omega}{\partial k}$ and this $\frac{\partial\omega}{\partial k}$ can be easily determined from the dispersion relation (15). It is also important to note that the stretched spatial variables perpendicular to the direction of magnetic field are different from the stretched spatial variable along the direction of propagation of the carrier wave because we have assumed that the carrier wave is propagating along the direction of the magnetic field.[46]

The physical quantities, viz., the ion number density (n), the electrostatic potential (ϕ), the ion fluid velocity parallel to the magnetic field (w), and the components of ion fluid velocity perpendicular to the magnetic field (u, v), are expanded into different harmonics of the fundamental IA carrier wave (k, $\omega(k)$) as

$$f=f^{(0)}+\sum_{l=1}^{\infty}\epsilon^l\sum_{a=-\infty}^{\infty}f_a^{(l)}(\xi,\eta,\zeta,\tau)\exp[ia\psi], \qquad (19)$$

$$s=s^{(0)}+\sum_{l=1}^{\infty}\epsilon^{l+1}\sum_{a=-\infty}^{\infty}s_a^{(l)}(\xi,\eta,\zeta,\tau)\exp[ia\psi], \qquad (20)$$

where $\psi=kz-\omega t$, k is the wave number, ω is the wave frequency, $f=n$, w, ϕ, and $s=u$, v with $n^{(0)}=1$, $u^{(0)}=v^{(0)}=w^{(0)}=0$, $\phi^{(0)}=0$. Here, we have also used the terminologies: $f_{-a}^{(l)}=\bar{f}_a^{(l)}$ and $s_{-a}^{(l)}=\bar{s}_a^{(l)}$, where "bar" denotes the complex conjugate.

As $s^{(0)}=0$, Eq. (20) shows that the perturbed velocity components of ion fluid (u and v) perpendicular to the direction of propagation of the wave are one order higher than the perturbed field variables along the direction of propagation of the wave.

To make a one-one correspondence between the multiple scale perturbation method[51,52] and the RPM,[30,31] we have the following consistency conditions:

$$(i)\ n_0^{(1)}=0,\quad u_0^{(1)}=v_0^{(1)}=w_0^{(1)}=0,\quad \phi_0^{(1)}=0, \qquad (21)$$

$$(ii)\ n_a^{(l)}=0,\quad u_a^{(l)}=v_a^{(l)}=w_a^{(l)}=0,\quad \phi_a^{(l)}=0\ \text{ for }\ l<|a|. \qquad (22)$$

Again, in the perturbation expansions (19) and (20), there is only one term corresponding to $a=0$ and also for $-a=0$, and consequently, without loss of generality, we can assume $\bar{f}_0^{(l)}=\bar{s}_0^{(l)}=0$ for any admissible value of l.

Substituting the perturbation expansions for n, u, v, w, and ϕ, according to the law as given in (19) and (20), into the Eqs. (1), (2), (4), and (11) and collecting the terms of different powers of ϵ, we get a sequence of equations of different orders. From each equation of a particular order, one can generate another sequence of equations for different harmonics by changing the values of a.

A. First Order: O(ϵ)=1

It is simple to check that the zeroth harmonic ($a=0$) equations for the continuity equation of ions, the z-component of equation of motion of ions and the Poisson equation are identically satisfied due to the consistency condition (21). So, at this order, we shall first of all consider the equations of first harmonic ($a=1$).

Solving the first harmonic ($a = 1$) equations of the continuity equation of ions and the z-component of equation of motion of ions for the unknowns $n_1^{(1)}$ and $w_1^{(1)}$, we get

$$n_1^{(1)} = \frac{k^2}{W^2}\phi_1^{(1)}, \quad w_1^{(1)} = \frac{k\omega}{W^2}\phi_1^{(1)}, \tag{23}$$

where $W^2 = \omega^2 - \sigma\gamma k^2$.

From the first harmonic ($a = 1$) equation of the Poisson equation, we get

$$n_1^{(1)} = (k^2 + h_1)\phi_1^{(1)}. \tag{24}$$

This equation and the first equation of (23) give the following linearized dispersion relation of IA waves

$$\frac{\omega^2}{k^2} = \frac{1}{k^2 + h_1} + \gamma\sigma. \tag{25}$$

This equation is exactly same as the Eq. (15).

B. Second order: O(ϵ)=2

1. First harmonic (a = 1)

Solving the first harmonic ($a = 1$) equations of the continuity equation of ions and the z-component of equation of motion of ions for the unknowns $n_1^{(2)}$ and $w_1^{(2)}$, we get

$$n_1^{(2)} = \frac{k^2}{W^2}\phi_1^{(2)} + \frac{2ik\omega(V_g k - \omega)}{W^4}\frac{\partial\phi_1^{(1)}}{\partial\zeta}, \tag{26}$$

$$w_1^{(2)} = \frac{k\omega}{W^2}\phi_1^{(2)} + \frac{i(V_g k - \omega)(\omega^2 + \sigma\gamma k^2)}{W^4}\frac{\partial\phi_1^{(1)}}{\partial\zeta}. \tag{27}$$

Again, solving the first harmonic ($a = 1$) equations of the x-component and y-component of the equations of motion of the ion fluid for the unknowns $u_1^{(1)}$ and $v_1^{(1)}$, we get

$$u_1^{(1)} = \frac{\omega^2}{W^2(\omega_c^2 - \omega^2)}\left[i\omega\frac{\partial\phi_1^{(1)}}{\partial\xi} - \omega_c\frac{\partial\phi_1^{(1)}}{\partial\eta}\right], \tag{28}$$

$$v_1^{(1)} = \frac{\omega^2}{W^2(\omega_c^2 - \omega^2)}\left[i\omega\frac{\partial\phi_1^{(1)}}{\partial\eta} + \omega_c\frac{\partial\phi_1^{(1)}}{\partial\xi}\right]. \tag{29}$$

From the first harmonic ($a = 1$) equation of the Poisson equation, we get

$$n_1^{(2)} = (k^2 + h_1)\phi_1^{(2)} - 2ik\frac{\partial\phi_1^{(1)}}{\partial\zeta}. \tag{30}$$

Substituting expression (26) for $n_1^{(2)}$, in Eq. (30), we get

$$-\frac{k^2(k^2 + h_1)}{W^2}\left\{\frac{\omega^2}{k^2} - \left(\gamma\sigma + \frac{1}{k^2 + h_1}\right)\right\}\phi_1^{(2)} + \frac{2i\omega k^2}{W^4}\left(V_g - \frac{\omega^2 - W^4}{\omega k}\right)\frac{\partial\phi_1^{(1)}}{\partial\zeta} = 0. \tag{31}$$

The first term of this equation is equal to zero due to the linear dispersion relation (25) of IA waves and the second term of the above mentioned equation can be made equal to zero if

$$V_g = \frac{\omega^2 - W^4}{\omega k} = \frac{k}{\omega}\left[\frac{h_1}{(k^2 + h_1)^2} + \sigma\gamma\right], \tag{32}$$

where we have used the linear dispersion relation (25) to simplify the above mentioned equation.

Now, differentiating the linear dispersion relation (25) with respect to k, we get

$$\frac{\partial\omega}{\partial k} = \frac{k}{\omega}\left[\frac{h_1}{(k^2 + h_1)^2} + \sigma\gamma\right]. \tag{33}$$

From Eqs. (32) and (33), we get $V_g = \frac{\partial\omega}{\partial k}$, and consequently, Eq. (31) is identically satisfied if V_g is the group velocity of IA waves.

2. Second harmonic (a = 2)

Solving the second harmonic ($a = 2$) equations of the continuity equation of ions, the z-component of the equation of motion of ions and the Poisson equation for the unknowns $\phi_2^{(2)}$, $n_2^{(2)}$, and $w_2^{(2)}$, we get

$$(\phi_2^{(2)}, n_2^{(2)}, w_2^{(2)}) = (A_\phi, A_n, A_w)\left[\phi_1^{(1)}\right]^2, \tag{34}$$

where

$$A_\phi = -\frac{h_2}{3k^2} + \frac{k^2\omega^2}{2W^6} + \gamma g_1\sigma\frac{k^4}{6W^6}, \tag{35}$$

$$A_n = (4k^2 + h_1)A_\phi + h_2, \quad A_w = \frac{\omega}{k}\left[A_n - \frac{k^4}{W^4}\right], \tag{36}$$

$$g_1 = \gamma - 2. \tag{37}$$

3. Zeroth harmonic (a = 0)

Solving the zeroth harmonic ($a = 0$) equations of the continuity equation of ions, the z-component of the equation of motion of ions and the Poisson equation for the unknowns $\phi_0^{(2)}$, $n_0^{(2)}$, and $w_0^{(2)}$, we get

$$(\phi_0^{(2)}, n_0^{(2)}, w_0^{(2)}) = (B_\phi, B_n, B_w)|\phi_1^{(1)}|^2, \tag{38}$$

where

$$B_\phi = \frac{g_1\gamma\sigma k^4 + k^2\omega(2kV_g + \omega) - 2h_2W^4(V_g^2 - \gamma\sigma)}{W^4\left[h_1(V_g^2 - \sigma\gamma) - 1\right]}, \tag{39}$$

$$B_n = h_1B_\phi + 2h_2, \quad B_w = V_gB_n - \frac{2\omega k^3}{W^4}. \tag{40}$$

C. Third order (O(ϵ) = 3): First harmonic ($a = 1$)

Solving the continuity equation of ions and the z-component of the equation of motion of ions for the unknowns $n_1^{(3)}$ and $w_1^{(3)}$, we can express $n_1^{(3)}$ and $w_1^{(3)}$ as a function of $\phi_1^{(1)}$, $\phi_1^{(2)}$, and $\phi_1^{(3)}$ along with their different derivatives with respect to ξ, η, ζ, and τ. In particular, $n_1^{(3)}$ can be expressed as

$$n_1^{(3)} = \frac{k^2}{W^2}\phi_1^{(3)} + 2ik\frac{\omega(V_g k-\omega)}{W^4}\frac{\partial\phi_1^{(2)}}{\partial\zeta} - i\frac{2k^2\omega}{W^4}\frac{\partial\phi_1^{(1)}}{\partial\tau} + \frac{\omega^4}{W^4(\omega_c^2-\omega^2)}\left(\frac{\partial^2\phi_1^{(1)}}{\partial\xi^2}+\frac{\partial^2\phi_1^{(1)}}{\partial\eta^2}\right) - \frac{(V_g k-\omega)}{W^6}(3V_g k\omega^2 - 3\sigma\gamma k^2\omega - \omega^3 + \sigma\gamma V_g k^3)\frac{\partial^2\phi_1^{(1)}}{\partial\zeta^2} + \left[2\frac{k^3\omega}{W^4}(A_w+B_w) + \frac{k^2}{W^4}(\omega^2+\sigma\gamma g_1 k^2) \times (A_n+B_n) + \sigma\gamma g_2\frac{k^8}{W^8}\right]|\phi_1^{(1)}|^2\phi_1^{(1)}, \tag{41}$$

where $g_2 = \frac{(\gamma-2)(\gamma-3)}{2}$.

From the Poisson equation, we get

$$n_1^{(3)} = (k^2+h_1)\phi_1^{(3)} - 2ik\frac{\partial\phi_1^{(2)}}{\partial\zeta} - \frac{\partial^2\phi_1^{(1)}}{\partial\xi^2} - \frac{\partial^2\phi_1^{(1)}}{\partial\eta^2} - \frac{\partial^2\phi_1^{(1)}}{\partial\zeta^2} + \{2h_2(A_\phi+B_\phi)+3h_3\}|\phi_1^{(1)}|^2\phi_1^{(1)}. \tag{42}$$

Now, eliminating $n_1^{(3)}$ from Eqs. (42) and (41), we get

$$-\frac{k^2(k^2+h_1)}{W^2}\left\{\frac{\omega^2}{k^2} - \left(\gamma\sigma + \frac{1}{k^2+h_1}\right)\right\}\phi_1^{(3)} + \frac{2i\omega k^2}{W^4}\left(V_g - \frac{\omega^2-W^4}{\omega k}\right)\frac{\partial\phi_1^{(2)}}{\partial\zeta} - i\frac{2k^2\omega}{W^4}\frac{\partial\phi_1^{(1)}}{\partial\tau} + \left(\frac{\omega^4}{W^4(\omega_c^2-\omega^2)}+1\right)\left(\frac{\partial^2\phi_1^{(1)}}{\partial\xi^2}+\frac{\partial^2\phi_1^{(1)}}{\partial\eta^2}\right) + \left[1 - \frac{k^4\left(V_g-\frac{\omega}{k}\right)}{W^6}\left(3V_g\frac{\omega^2}{k^2} - 3\gamma\sigma\frac{\omega}{k} - \frac{\omega^3}{k^3} + \gamma\sigma V_g\right)\right] \times \frac{\partial^2\phi_1^{(1)}}{\partial\zeta^2} + \left[2\frac{k^3\omega}{W^4}(A_w+B_w) + \frac{k^2}{W^4}(\omega^2+\sigma\gamma g_1k^2) \times (A_n+B_n) + \sigma\gamma g_2\frac{k^8}{W^8} - 3h_3 - 2h_2(A_\phi+B_\phi)\right] \times |\phi_1^{(1)}|^2\phi_1^{(1)} = 0. \tag{43}$$

Using the linear dispersion relation (25) and the expression of V_g as given in Eq. (32), Eq. (43) can be written as

$$i\frac{\partial\phi_1^{(1)}}{\partial\tau} + P\frac{\partial^2\phi_1^{(1)}}{\partial\zeta^2} + Q|\phi_1^{(1)}|^2\phi_1^{(1)} - R\left(\frac{\partial^2\phi_1^{(1)}}{\partial\xi^2}+\frac{\partial^2\phi_1^{(1)}}{\partial\eta^2}\right) = 0, \tag{44}$$

where

$$P = -\frac{W^4}{2k^2\omega}\left[1 - \frac{k^4}{W^6}\left(V_g - \frac{\omega}{k}\right) \times \left(3V_g\frac{\omega^2}{k^2} - 3\gamma\sigma\frac{\omega}{k} - \frac{\omega^3}{k^3} + \gamma\sigma V_g\right)\right], \tag{45}$$

$$Q = -\frac{W^4}{2k^2\omega}\left[2\frac{k^3\omega}{W^4}(A_w+B_w) + \frac{k^2}{W^4}(\omega^2+\sigma\gamma g_1k^2) \times (A_n+B_n) + \sigma\gamma g_2\frac{k^8}{W^8} - 3h_3 - 2h_2(A_\phi+B_\phi)\right], \tag{46}$$

$$R = \frac{W^4}{2k^2\omega}\left[\frac{\omega^4}{W^4(\omega_c^2-\omega^2)}+1\right]. \tag{47}$$

IV. MODULATIONAL INSTABILITY

To study the stability of the modulated IA waves represented by the NLSE (44), we assume that the modulated IA wave [i.e., when modulation on the wave amplitude (packet) takes place[47]] is propagating along a direction having direction cosines (l_1, m_1, n_1), and consequently, we consider the transformation

$$\xi' = l_1\xi + m_1\eta + n_1\zeta, \quad \tau' = \tau, \tag{48}$$

where $l_1^2 + m_1^2 + n_1^2 = 1$.

Substituting (48) in Eq. (44) and dropping the prime from the independent variables ξ' and τ', we get the following one dimensional NLSE:

$$i\frac{\partial\phi_1^{(1)}}{\partial\tau} + P_1\frac{\partial^2\phi_1^{(1)}}{\partial\xi^2} + Q|\phi_1^{(1)}|^2\phi_1^{(1)} = 0, \tag{49}$$

where

$$P_1 = Pn_1^2 - R(l_1^2+m_1^2) = (P+R)n_1^2 - R. \tag{50}$$

Now, it is simple to check that $\phi_1^{(1)} = \phi_0 e^{i\Delta\tau}$ is a steady state solution of the NLSE (49) if $\Delta = Q|\phi_0|^2$, where ϕ_0 is a constant.

To study the MI of IA waves, we decompose $\phi_1^{(1)}$ as

$$\phi_1^{(1)} = (\phi_0 + \delta\phi)e^{i\Delta\tau} \quad \text{where } |\delta\phi| \ll |\phi_0|. \tag{51}$$

Substituting (51) into Eq. (49) and finally linearizing the equation with respect to the perturbed quantity $\delta\phi$, we get the following equation:

$$i\frac{\partial\delta\phi}{\partial\tau} + P_1\frac{\partial^2\delta\phi}{\partial\xi^2} + Q|\phi_0|^2(\delta\phi + \overline{\delta\phi}) = 0, \tag{52}$$

where $\overline{\delta\phi}$ is the complex conjugate of $\delta\phi$.

Substituting $\delta\phi = U + iV$ into Eq. (52) and then separating into real and imaginary parts, we obtain the following two coupled equations:

$$-\frac{\partial V}{\partial\tau} + P_1\frac{\partial^2 U}{\partial\xi^2} + 2QU|\phi_0|^2 = 0, \tag{53}$$

$$\frac{\partial U}{\partial\tau} + P_1\frac{\partial^2 V}{\partial\xi^2} = 0, \tag{54}$$

where we have assumed that U and V are real functions of ξ and τ.

Substituting

$$U = U_0\exp[i(K\xi - \Omega\tau)] + c.c., \tag{55}$$

$$V = V_0\exp[i(K\xi - \Omega\tau)] + c.c., \tag{56}$$

into Eqs. (53) and (54), we get the following equations:

$$i\Omega V_0 + (-P_1K^2 + 2Q|\phi_0|^2)U_0 = 0, \tag{57}$$

$$i\Omega U_0 + P_1K^2V_0 = 0. \tag{58}$$

For the nontrivial solution of the above linear equations for the unknown quantities U_0 and V_0, we get

$$\Omega^2 = \left[P_1K^2\right](P_1K^2 - 2Q|\phi_0|^2). \tag{59}$$

If $1 - \frac{2Q|\phi_0|^2}{P_1K^2} \geq 0$, then from (59), one can get real values of Ω, and consequently, IA wave is modulationally stable. From the expression of Ω^2 as given in Eq. (59), we see that Ω^2 is strictly positive for $P_1Q < 0$. Therefore, the IA wave is always modulationally stable for all $P_1Q < 0$. On the other hand, if $P_1Q > 0$, then $\Omega^2 \geq 0$ or $\Omega^2 < 0$ according to whether $K \geq K_c$ or $K < K_c$, where $K_c = \sqrt{\frac{2Q|\phi_0|^2}{P_1}}$. Therefore, we see that IA wave is modulationally stable, i.e., $\Omega^2 \geq 0$ when either $P_1Q < 0$ or $K \geq K_c$ whenever $P_1Q > 0$. On the other hand, if $P_1Q > 0$ and $K < K_c$, then $\Omega^2 < 0$ and all the roots of Eq. (59) for the unknown Ω are purely imaginary. Consequently, the IA wave is modulationally unstable and the growth rate of instability Γ $(= Im(\Omega))$ is given by the following equation:

$$\Gamma^2 = \left[P_1K^2\right]^2 \left[\frac{2Q|\phi_0|^2}{P_1K^2} - 1\right]. \tag{60}$$

For given values of P_1 and Q, the growth rate of instability Γ attains its maximum value Γ_{max} at $K = \frac{K_c}{\sqrt{2}} = \sqrt{\frac{Q|\phi_0|^2}{P_1}}$ and the maximum growth rate of instability Γ_{max} is given by

$$\Gamma_{max} = |Q||\phi_0|^2. \tag{61}$$

From Eq. (59), we see that $\Omega^2 = 0$ if $P_1 = 0$. Although we see that $\Omega^2 = [P_1K^2]^2$, if $Q = 0$, the analysis is erroneous because for $Q = 0$, it is not possible to study the MI of IA waves with the help of the present NLSE. For $Q = 0$, Eq. (49) loses its nonlinearity and consequently, a modified NLSE is necessary to study the MI of IA waves.

Again, from the expressions of Q and P_1 as given by Eqs. (46) and (50), respectively, we see that Q is independent of l_1, m_1, n_1 whereas P_1 depends only on n_1 for the fixed value of the other parameters of the system. Now, if δ is the angle of propagation of the modulated IA wave with the external uniform static magnetic field directed along z-axis, then $n_1 = \cos\delta$. Therefore, for the given set of values of the parameters, the stability of the modulated IA waves depends only on δ.

V. SUMMARY AND DISCUSSIONS

In the present paper, we have considered the MI of IA waves in a magnetized collisionless plasma consisting of adiabatic warm ions and two species of electrons at different temperatures, a cooler one with a Boltzmann distribution and a hotter one with a nonthermal Cairns distribution, immersed in a uniform static magnetic field directed along z-axis. Using RPM,[30,31] a three dimensional NLSE has been derived to study the instability of the modulated IA waves. The instability condition and the maximum growth rate of instability have been investigated with respect to any parameter of the present plasma system.

It is simple to check that the phase velocity and the group velocity are decreasing functions of k for any set of values of the parameters involved in the system. At $k = 4$, the phase velocity and the group velocity of the IA wave assume a very small numerical value, and consequently, the value of k is restricted by $0 < k < 4$.

It is easy to check that P_1Q is a function of k, β_e, n_{sc}, σ_{sc}, ω_c, n_1, σ, and γ. Therefore, P_1Q can be taken as a function of k and β_e for fixed values of the other parameters n_{sc}, σ_{sc}, ω_c, n_1, σ, and γ. Consequently, $P_1Q = 0$ gives a functional relationship between k and β_e. This functional relation between k and β_e is plotted in Fig. 1 for fixed values of the other parameters as mentioned in Fig. 1. From Fig. 1, we see that in the interval $0.262 \leq k \leq 0.316$, there is no functional relation between k and β_e for which $P_1Q = 0$. Here, we have used the terminology N to indicate that we are unable to determine the functional relationship between k and β_e for which $P_1Q = 0$ for the entire indicated rectangular region enclosed by $0.262 \leq k \leq 0.316$ and $0 \leq \beta_e \leq 0.6$. In fact, there is a singularity of the function P_1Q at a point $k = k_\beta$ lying within the interval $0.262 \leq k \leq 0.316$ for any given value of β_e. To explain the behaviour of P_1Q as a function of k only for given value of β_e lying within the interval $0 \leq \beta_e \leq 0.6$, we draw Fig. 2 in the indicated region of k for two different values of β_e. Figure 2 clearly shows $P_1Q \neq 0$ for $0.262 \leq k \leq 0.316$ with $\beta_e = 0.3$ and $\beta_e = 0.5$. In fact, it can be easily checked that $P_1Q \neq 0$ for any k lying within the interval $0.262 \leq k \leq 0.316$ and for any β_e lying within the interval $0 \leq \beta_e \leq 0.6$. From Fig. 2(a) [Fig. 2(b)], we see that P_1Q has a singularity at the point $k = k_\beta = 0.28981$ (0.27199) (approx.). As $P_1Q \neq 0$ in the interval $0.262 \leq k \leq 0.316$ for any physically admissible value of β_e, we are unable to draw the functional relationship between β_e and k within the interval $0.262 \leq k \leq 0.316$. But from Fig. 2, it is evident that $P_1Q < 0$ for $0.262 \leq k < k_\beta$ whereas $P_1Q > 0$ for $k_\beta < k \leq 0.316$. So, from Figs. 1 and 2, we can conclude that there exists a region (an interval or union of more than one intervals) of k such that $P_1Q < 0$ for any set of given values of the parameters and consequently, IA waves are modulationally stable in that region of k.

In Figs. 3(a), 3(b), and 3(c), β_e is plotted against k when $P_1Q = 0$ for $\omega_c = 0.2$, $\omega_c = 0.5$, and $\omega_c = 0.8$, respectively. From Fig. 3, we see that the region presented by N

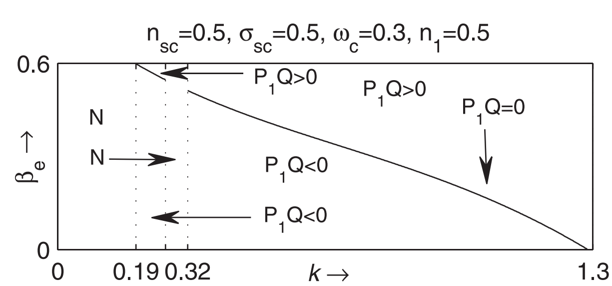

FIG. 1. β_e is plotted against k when $P_1Q = 0$ for $\gamma = 5/3$ and $\sigma = 0.001$.

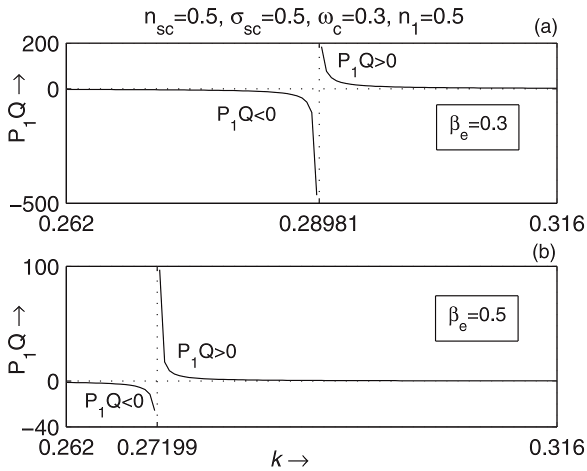

FIG. 2. P_1Q is plotted against k for (a) $\beta_e = 0.3$ and (b) $\beta_e = 0.5$.

increases with increasing ω_c. We see that the existence of both stable and unstable modulated IA waves is confirmed.

In Fig. 4, the functional relationship between k and β_e is plotted when $P_1Q = 0$ for different values of n_1. From this figure, we can conclude that the region N increases with increasing n_1 and the existence of both stable and unstable modulated IA waves is confirmed.

Again, P_1Q can be considered as a function of k and n_1 for fixed values of n_{sc}, σ_{sc}, β_e, ω_c, σ, γ, and consequently, $P_1Q = 0$ gives a functional relationship between k and n_1. This functional relationship between k and n_1 is plotted in Figs. 5–9, for different values of ω_c with $\beta_e = 0$, for different values of ω_c with $\beta_e = 0.3$, for different values of β_e, for different values of n_{sc}, and for different values of σ_{sc}, respectively.

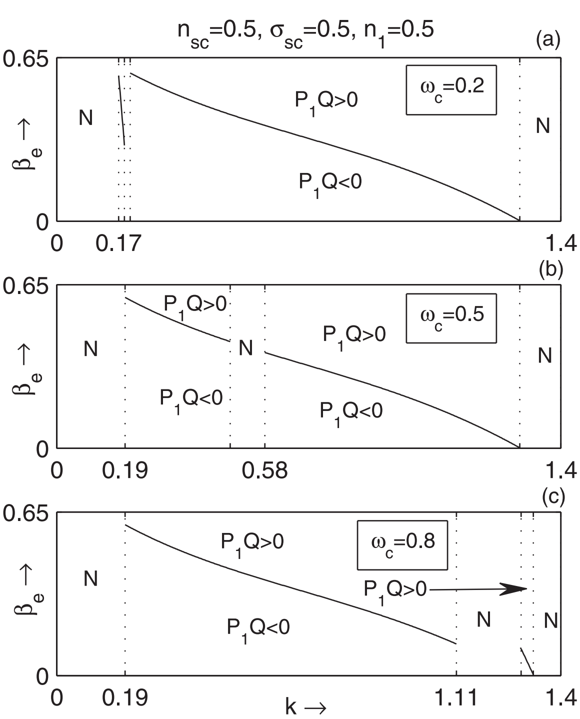

FIG. 3. β_e is plotted against k when $P_1Q = 0$ for different values of ω_c: (a) $\omega_c = 0.2$, (b) $\omega_c = 0.5$, and (c) $\omega_c = 0.8$, when $\gamma = 5/3$ and $\sigma = 0.001$.

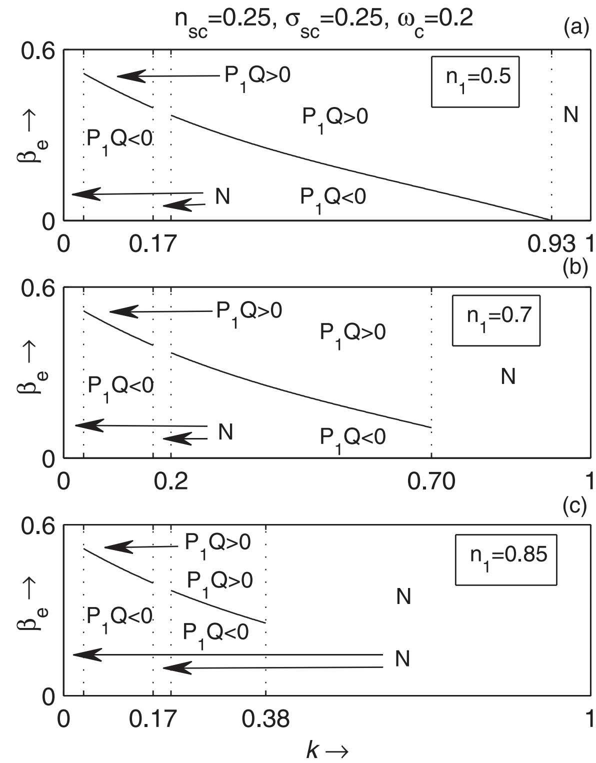

FIG. 4. β_e is plotted against k when $P_1Q = 0$ for different values of n_1: (a) $n_1 = 0.5$, (b) $n_1 = 0.7$, and (c) $n_1 = 0.85$, when $\gamma = 5/3$ and $\sigma = 0.001$.

When both the electron species are isothermally distributed, then we have $\beta_e = 0$, and for this case, in Fig. 5, n_1 is plotted against k when $P_1Q = 0$ for (a) $\omega_c = 0.01$, (b) $\omega_c = 0.2$, (c) $\omega_c = 0.4$, and (d) $\omega_c = 0.6$. From Fig. 5, we see that both the regions $P_1Q > 0$ and $P_1Q < 0$ are bounded. For example, the region $P_1Q > 0$ of Fig. 5(a) is bounded by the curves $n_1 = 1$ and $P_1Q = 0$, whereas the region $P_1Q < 0$ of Fig. 5(a) is bounded by the curves $k = 0$, $k = 3.817$, $n_1 = 0$ and $P_1Q = 0$. Figure 5 shows that IA waves are

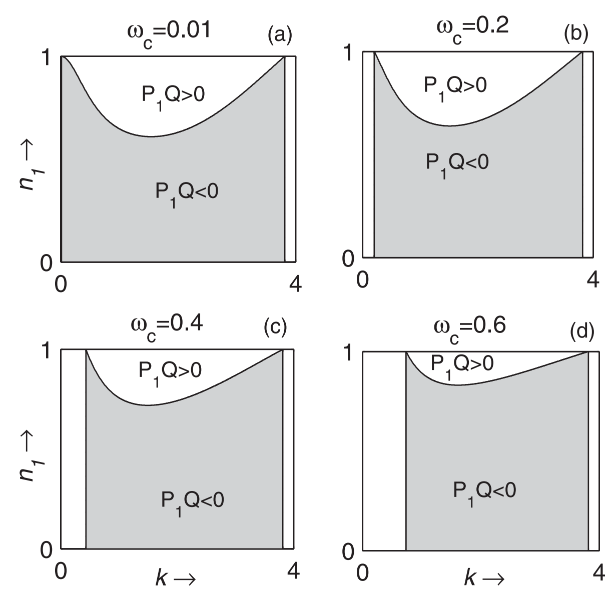

FIG. 5. n_1 is plotted against k when $P_1Q = 0$ for different values of ω_c: (a) $\omega_c = 0.01$, (b) $\omega_c = 0.2$, (c) $\omega_c = 0.4$, and (d) $\omega_c = 0.6$, and $\gamma = 5/3$, $\sigma = 0.001$, $\beta_e = 0$, $n_{sc} = 0.25$, and $\sigma_{sc} = 0.25$.

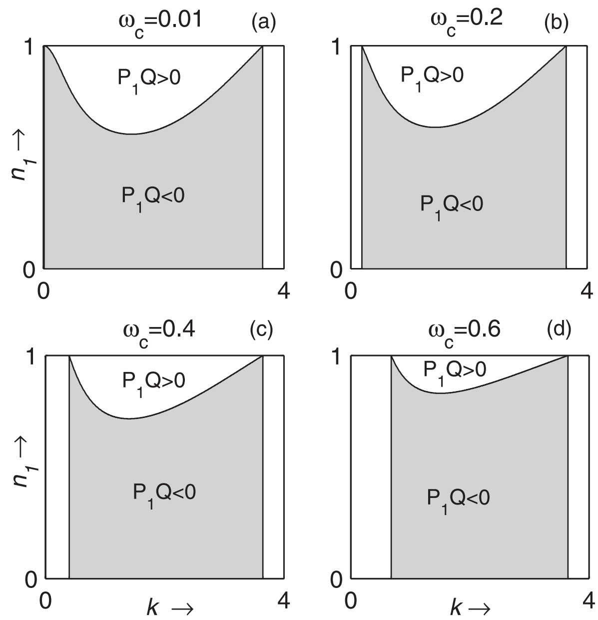

FIG. 6. n_1 is plotted against k when $P_1Q = 0$ for different values of ω_c: (a) $\omega_c = 0.01$, (b) $\omega_c = 0.2$, (c) $\omega_c = 0.4$, and (d) $\omega_c = 0.6$, and $\gamma = 5/3$, $\sigma = 0.001$, $\beta_e = 0.3$, $n_{sc} = 0.25$, and $\sigma_{sc} = 0.25$.

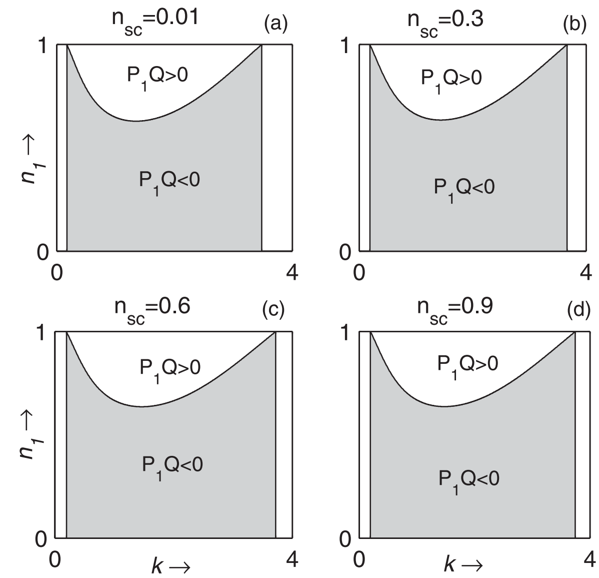

FIG. 8. n_1 is plotted against k when $P_1Q = 0$ for different values of n_{sc}: (a) $n_{sc} = 0.01$, (b) $n_{sc} = 0.3$, (c) $n_{sc} = 0.6$, and (d) $n_{sc} = 0.9$, and $\gamma = 5/3$, $\sigma = 0.001$, $\beta_e = 0.3$, $\sigma_{sc} = 0.25$, and $\omega_c = 0.2$.

modulationally stable for any point (k, n_1) lying within the shaded regions of Fig. 5. Again, for any point (k, n_1) lying within region $P_1Q > 0$, IA waves are modulationally stable or unstable according to whether $K > K_c$ or $K < K_c$. Figure 5 shows that the interval of k for which modulated IA waves are stable decreases with increasing ω_c. It is simple to check that the stable region of modulated IA waves increases with increasing σ.

In Fig. 6, n_1 is plotted against k when $P_1Q = 0$ for (a) $\omega_c = 0.01$, (b) $\omega_c = 0.2$, (c) $\omega_c = 0.4$, and (d) $\omega_c = 0.6$ with $\beta_e = 0.3$. From this figure, one can draw the same conclusion as given in Fig. 5. Basically, there is no qualitative change between Figs. 5 and 6. Here also IA waves are modulationally stable for any point (k, n_1) lying within the shaded regions of Fig. 6. On the other hand, IA waves are modulationally stable or unstable according to whether $K > K_c$ or $K < K_c$ for any point (k, n_1) lying within region $P_1Q > 0$. The region $P_1Q > 0$ decreases with increasing ω_c, i.e., instability of IA wave decreases with increasing ω_c. It is simple to check that the stable region of modulated IA waves increases with increasing ion temperature.

In Fig. 7, n_1 is plotted against k when $P_1Q = 0$ for different values of β_e, viz., (a) $\beta_e = 0$, (b) $\beta_e = 0.2$, (c) $\beta_e = 0.4$, and (d) $\beta_e = 0.6$. From Fig. 7, we see that both the

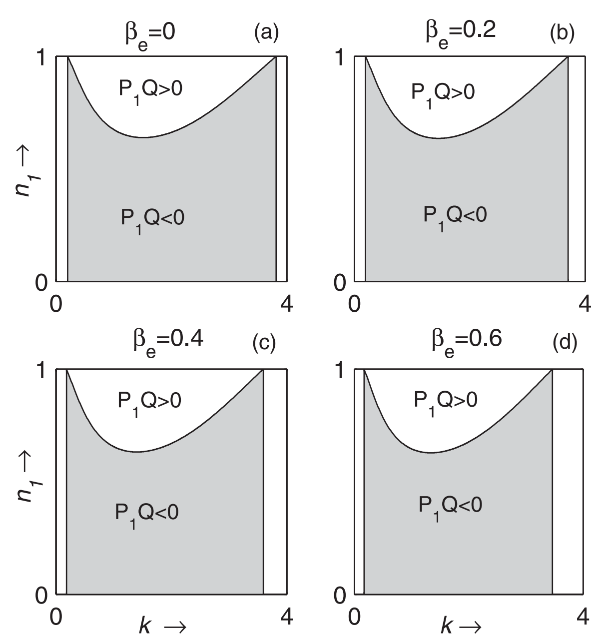

FIG. 7. n_1 is plotted against k when $P_1Q = 0$ for different values of β_e: (a) $\beta_e = 0$, (b) $\beta_e = 0.2$, (c) $\beta_e = 0.4$, and (d) $\beta_e = 0.6$, and $\gamma = 5/3$, $\sigma = 0.001$, $\omega_c = 0.2$, $n_{sc} = 0.25$, and $\sigma_{sc} = 0.25$.

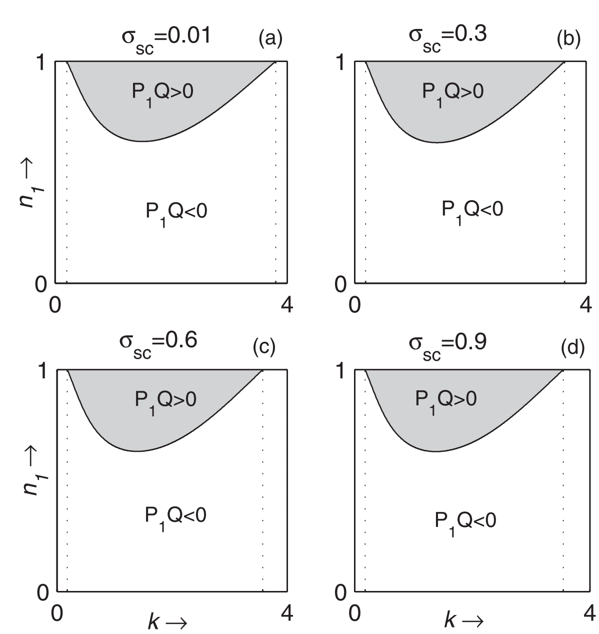

FIG. 9. n_1 is plotted against k when $P_1Q = 0$ for different values of σ_{sc}: (a) $\sigma_{sc} = 0.01$, (b) $\sigma_{sc} = 0.3$, (c) $\sigma_{sc} = 0.6$, and (d) $\sigma_{sc} = 0.9$, and $\gamma = 5/3$, $\sigma = 0.001$, $\beta_e = 0.3$, $n_{sc} = 0.25$, and $\omega_c = 0.2$.

regions $P_1Q > 0$ and $P_1Q < 0$ are slowly decreasing with increasing β_e. One can easily check that stable region increases with increasing σ.

In Fig. 8, n_1 is plotted against k when $P_1Q = 0$ for different values of n_{sc}, viz., (a) $n_{sc} = 0.01$, (b) $n_{sc} = 0.3$, (c) $n_{sc} = 0.6$, and (d) $n_{sc} = 0.9$. From Fig. 8, we see that the region $P_1Q < 0$ is slowly increasing with increasing n_{sc}, and consequently, the stable region slowly increases with increasing n_{sc}.

In Fig. 9, n_1 is plotted against k when $P_1Q = 0$ for different values of σ_{sc}, viz., (a) $\sigma_{sc} = 0.01$, (b) $\sigma_{sc} = 0.3$, (c) $\sigma_{sc} = 0.6$, and (d) $\sigma_{sc} = 0.9$. From Fig. 9, we see that the region $P_1Q < 0$ is slowly decreasing with increasing σ_{sc}, and consequently, the stable region slowly decreases with increasing σ_{sc}.

From Figs. 5–9, we see that for given set of values of the parameters, the modulated IA waves are stable in a right small neighbourhood of $n_1 = 0$ for any value of k lying within the interval $0 < k < 4$, i.e., for any small value of n_1, it is simple to check that IA waves are modulationally stable. However, from the above mentioned figures, we see that IA waves are modulationally stable for $0 \le n_1 \le 0.5 \Longleftrightarrow 0 \le \cos\delta \le 0.5 \Longleftrightarrow \cos\frac{\pi}{2} \le \cos\delta \le \cos\frac{\pi}{3} \Longleftrightarrow \frac{\pi}{2} \ge \delta \ge \frac{\pi}{3} \Longleftrightarrow \frac{\pi}{3} \le \delta \le \frac{\pi}{2}$. Therefore, for modulationally stable IA waves, we have $\frac{\pi}{3} \le \delta \le \frac{\pi}{2}$ (approximately). On the other hand, if $0 \le \delta \le \delta^{(c)}$, then IA waves are modulationally stable or unstable according to whether $K \ge K_c$ or $K < K_c$, where $\delta^{(c)}$ is a cut off value of δ which depends on the parameters of the system.

Now we analyze the maximum growth rate of instability (Γ_{max}) numerically with the help of Figs. 10–14. For this purpose, we shall first explain Fig. 10. Here, P_1, Q, and $\Gamma_{max}/|\phi_0|^2$ are plotted against k in Figs. 10(a), 10(b), and 10(c), respectively. From Fig. 10, we see that the maximum growth of instability exists in the intervals $0.204 < k < 0.836$ and $0.928 < k < 2$ as $P_1 > 0$ and $Q > 0$, i.e., $P_1Q > 0$ for

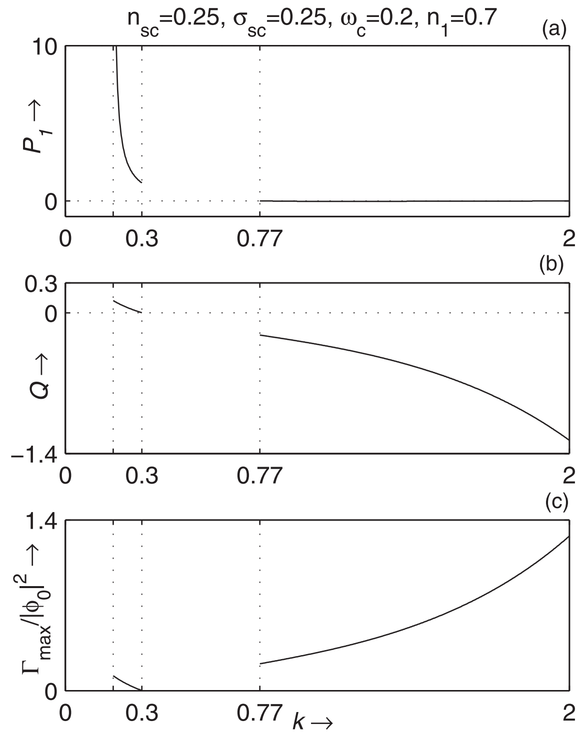

FIG. 11. P_1, Q, and $\Gamma_{max}/|\phi_0|^2$ are plotted against k in (a), (b), and (c), respectively, for $\beta_e = 0.3$, $\gamma = 5/3$, and $\sigma = 0.001$.

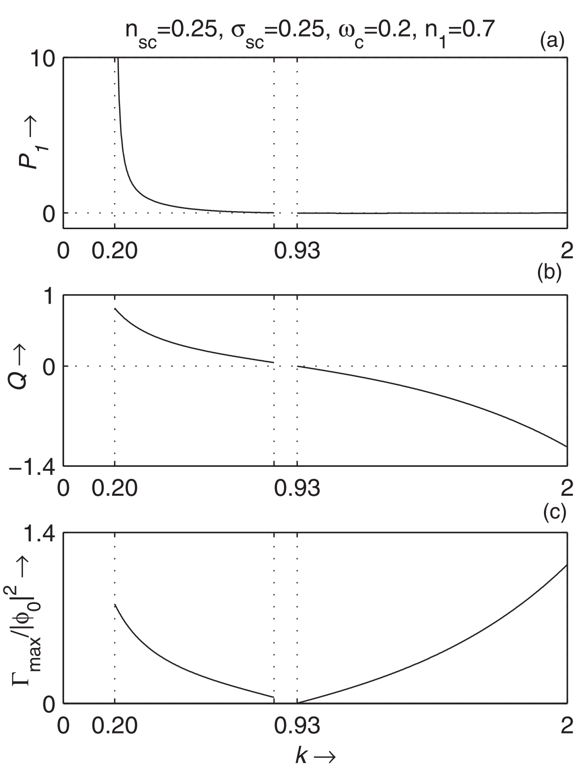

FIG. 10. P_1, Q, and $\Gamma_{max}/|\phi_0|^2$ are plotted against k in (a), (b), and (c), respectively, for $\beta_e = 0$, $\gamma = 5/3$, and $\sigma = 0.001$.

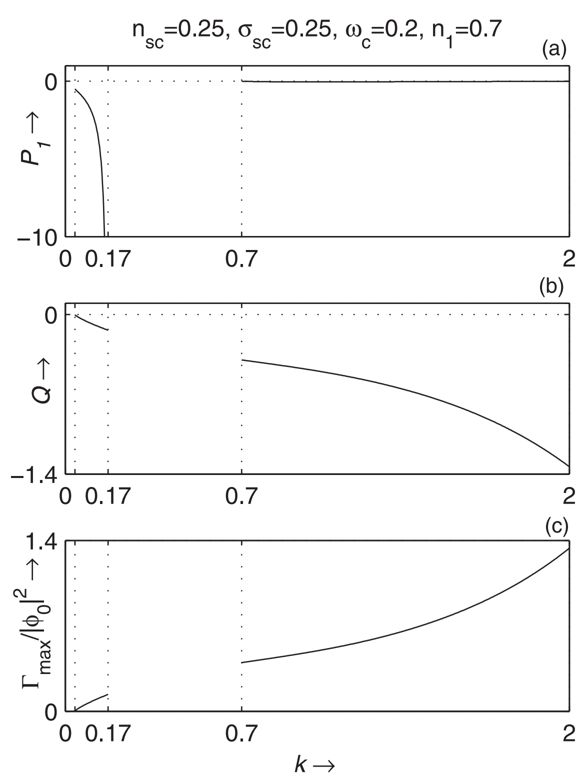

FIG. 12. P_1, Q, and $\Gamma_{max}/|\phi_0|^2$ are plotted against k in (a), (b), and (c), respectively, for $\beta_e = 0.6$, $\gamma = 5/3$, and $\sigma = 0.001$.

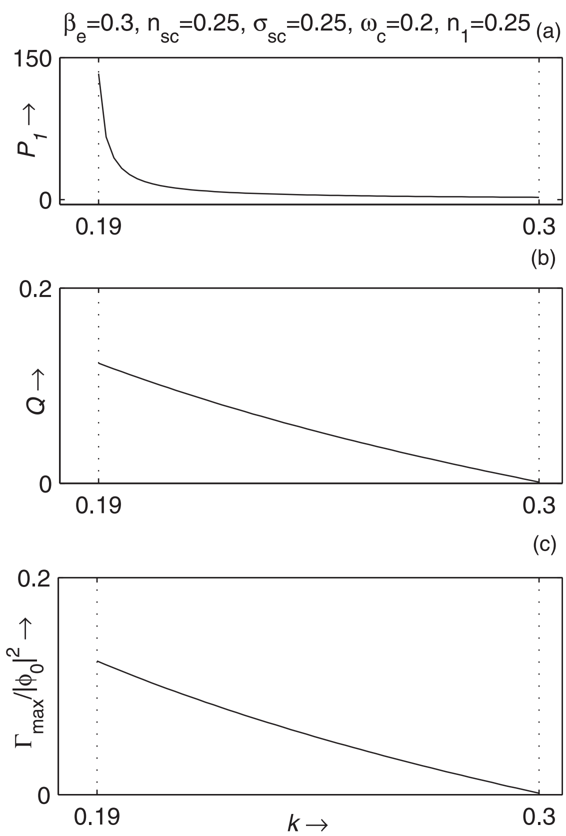

FIG. 13. P_1, Q, and $\Gamma_{max}/|\phi_0|^2$ are plotted against k in (a), (b), and (c), respectively, for $\gamma = 5/3$ and $\sigma = 0.001$.

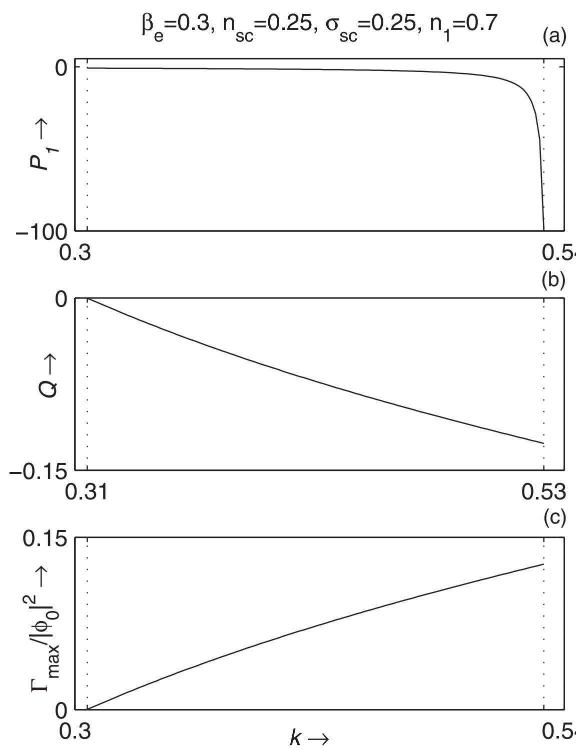

FIG. 14. P_1, Q, and $\Gamma_{max}/|\phi_0|^2$ are plotted against k in (a), (b), and (c), respectively, for $\omega_c = 0.5$, $\gamma = 5/3$, and $\sigma = 0.001$.

$0.204 < k < 0.836$, and $P_1 < 0$ and $Q < 0$, i.e., $P_1 Q > 0$ for $0.928 < k < 2$. On the other hand, within the interval $0.837 < k < 0.928$, $P_1 Q < 0$, which shows that the modulated IA wave is stable for $0.837 < k < 0.928$.

Similarly, from Fig. 11, we see that the maximum growth of instability exists for $0.190 < k < 0.304$ and $0.772 < k < 2$ as $P_1 Q > 0$ for all $0.190 < k < 0.304$ and $0.772 < k < 2$. For all values of k lying within the interval $0.304 < k < 0.771$, $P_1 Q < 0$, and consequently, the modulated IA wave is stable in this interval of k.

Finally, from Fig. 12, we see that the maximum growth of instability exists for all k lying within $0.038 < k < 0.17$ and $0.7 < k < 2$ whereas for $0.171 < k < 0.7$, $P_1 Q < 0$, and consequently, the modulated IA wave is stable for all k lying within $0.171 < k < 0.7$.

From Figs. 10(c), 11(c), and 12(c), we see that the region of existence of maximum growth rate of instability decreases with increasing β_e whereas the maximum growth rate of instability increases with increasing β_e.

P_1, Q, and $\Gamma_{max}/|\phi_0|^2$ are plotted against k in Figs. 13(a), 13(b), and 13(c), respectively. From Fig. 13, we see that the maximum growth of instability exists in the interval $0.19 < k < 0.304$ as $P_1 > 0$ and $Q > 0$ for $0.19 < k < 0.304$.

In Figs. 13(c) and 11(c), $\Gamma_{max}/|\phi_0|^2$ are plotted against k for $n_1 = 0.25$ and for $n_1 = 0.7$. Figures 13 and 11 are characteristically different. If $0 \le n_1 < 0.594$, then we have Fig. 13 and if $0.595 < n_1 < 1$ then we have Fig. 11.

From Figs. 13(c) and 11(c), we can conclude that the region of existence of maximum growth rate of instability increases with increasing n_1 whereas the maximum growth rate of instability remains unchanged within the common region of k ($0.190 < k < 0.304$).

Again, P_1, Q, and $\Gamma_{max}/|\phi_0|^2$ are plotted against k in Figs. 14(a), 14(b), and 14(c), respectively. From Fig. 14, we see that the maximum growth rate of instability exists in the interval $0.306 < k < 0.530$ as in the interval $0.306 < k < 0.530$, $P_1 < 0$ and $Q < 0$.

In Figs. 11(c) and 14(c), $\Gamma_{max}/|\phi_0|^2$ are plotted against k for different values of ω_c. Figures 11 and 14 correspond to $\omega_c = 0.2$ and $\omega_c = 0.5$, respectively. Figures 11 and 14 are characteristically different. If $0 < \omega_c < 0.406$, one can get a figure of type Fig. 11, whereas if $0.407 < \omega_c < 0.6$, one can get a figure of type Fig. 14. From these figures, we can conclude that the region of existence of maximum growth rate of instability decreases with increasing ω_c.

Again, from Figs. 10–14, we see that Γ_{max} increases or decreases with increasing k according to whether $Q < 0$ or $Q > 0$.

ACKNOWLEDGMENTS

The authors are grateful to the referee for extremely helpful comments, without which this paper could not have been written in its present form.

[1]R. E. Ergun, C. W. Carlson, J. P. McFadden, F. S. Mozer, G. T. Delory, W. Peria, C. C. Chaston, M. Temerin, R. Elphic, R. Strangeway *et al.*, Geophys. Res. Lett. **25**, 2025, doi:10.1029/98GL00635 (1998).
[2]R. E. Ergun, C. W. Carlson, J. P. McFadden, F. S. Mozer, G. T. Delory, W. Peria, C. C. Chaston, M. Temerin, R. Elphic, R. Strangeway *et al.*, Geophys. Res. Lett. **25**, 2061, doi:10.1029/98GL00570 (1998).
[3]G. T. Delory, R. E. Ergun, C. W. Carlson, L. Muschietti, C. C. Chaston, W. Peria, J. P. McFadden, and R. Strangeway, Geophys. Res. Lett. **25**, 2069, doi:10.1029/98GL00705 (1998).

[4]R. Pottelette, R. E. Ergun, R. A. Treumann, M. Berthomier, C. W. Carlson, J. P. McFadden, and I. Roth, Geophys. Res. Lett. **26**, 2629, doi:10.1029/1999GL900462 (1999).
[5]J. P. McFadden, C. W. Carlson, R. E. Ergun, F. S. Mozer, L. Muschietti, I. Roth, and E. Moebius, J. Geophys. Res. **108**, 8018, doi:10.1029/2002JA009485 (2003).
[6]R. Boström, G. Gustafsson, B. Holback, G. Holmgren, H. Koskinen, and P. Kintner, Phys. Rev. Lett. **61**, 82 (1988).
[7]R. Boström, IEEE Trans. Plasma Sci. **20**, 756 (1992).
[8]M. Temerin, K. Cerny, W. Lotko, and F. S. Mozer, Phys. Rev. Lett. **48**, 1175 (1982).
[9]H. Matsumoto, H. Kojima, T. Miyatake, Y. Omura, M. Okada, I. Nagano, and M. Tsutsui, Geophys. Res. Lett. **21**, 2915, doi:10.1029/94GL01284 (1994).
[10]J. R. Franz, P. M. Kintner, and J. S. Pickett, Geophys. Res. Lett. **25**, 1277, doi:10.1029/98GL50870 (1998).
[11]C. A. Cattell, J. Dombeck, J. R. Wygant, M. K. Hudson, F. S. Mozer, M. A. Temerin, W. K. Peterson, C. A. Kletzing, C. T. Russell, and R. F. Pfaff, Geophys. Res. Lett. **26**, 425, doi:10.1029/1998GL900304 (1999).
[12]P. O. Dovner, A. I. Eriksson, R. Boström, and B. Holback, Geophys. Res. Lett. **21**, 1827, doi:10.1029/94GL00886 (1994).
[13]R. A. Cairns, A. A. Mamum, R. Bingham, R. Boström, R. O. Dendy, C. M. C. Nairn, and P. K. Shukla, Geophys. Res. Lett. **22**, 2709, doi:10.1029/95GL02781 (1995).
[14]R. A. Cairns, A. A. Mamun, R. Bingham, and P. K. Shukla, Phys. Scr. **T63**, 80 (1996).
[15]A. A. Mamun and R. A. Cairns, J. Plasma Phys. **56**, 175 (1996).
[16]A. Bandyopadhyay and K. P. Das, Phys. Plasmas **9**, 465 (2002).
[17]S. A. Islam, A. Bandyopadhyay, and K. P. Das, J. Plasma Phys. **74**, 765 (2008).
[18]O. R. Rufai, R. Bharuthram, S. V. Singh, and G. S. Lakhina, Phys. Plasmas **21**, 082304 (2014).
[19]B. N. Goswami and B. Buti, Phys. Lett. A **57**, 149 (1976).
[20]K. Nishihara and M. Tajiri, J. Phys. Soc. Jpn. **50**, 4047 (1981).
[21]Yashvir, T. N. Bhatnagar, and S. R. Sharma, J. Plasma Phys. **33**, 209 (1985).
[22]R. Bharuthram and P. K. Shukla, Phys. Fluids **29**, 3214 (1986).
[23]S. Baboolal, R. Bharuthram, and M. A. Hellberg, J. Plasma Phys. **40**, 163 (1988).
[24]S. Baboolal, R. Bharuthram, and M. A. Hellberg, J. Plasma Phys. **41**, 341 (1989).
[25]S. Baboolal, R. Bharuthram, and M. A. Hellberg, J. Plasma Phys. **44**, 1 (1990).
[26]L. L. Yadav, R. S. Tiwari, and S. R. Sharma, J. Plasma Phys. **51**, 355 (1994).
[27]L. L. Yadav, R. S. Tiwari, K. P. Maheshwari, and S. R. Sharma, Phys. Rev. E **52**, 3045 (1995).
[28]S. G. Tagare, Phys. Plasmas **7**, 883 (2000).
[29]S. Dalui, A. Bandyopadhyay, and K. P. Das, Phys. Plasmas **24**, 042305 (2017).
[30]T. Taniuti and N. Yajima, J. Math. Phys. **10**, 1369 (1969).
[31]N. Asano, T. Taniuti, and N. Yajima, J. Math. Phys. **10**, 2020 (1969).
[32]I. Kourakis and P. K. Shukla, J. Phys. A **36**, 11901 (2003).
[33]A. Esfandyari-Kalejahi and H. Asgari, Phys. Plasmas **12**, 102302 (2005).
[34]A. Esfandyari-Kalejahi, I. Kourakis, and M. Akbari-Moghanjoughi, J. Plasma Phys. **76**, 169 (2010).
[35]H. Alinejad, M. Mahdavi, and M. Shahmansouri, Astrophys. Space Sci. **352**, 571 (2014).
[36]S. Sultana, S. Islam, and A. A. Mamun, Astrophys. Space Sci. **351**, 581 (2014).
[37]Shalini, N. S. Saini, and A. P. Misra, Phys. Plasmas **22**, 092124 (2015).
[38]M. Kako, Prog. Theor. Phys. Suppl. **55**, 120 (1974).
[39]G. Murtaza and M. Salahuddin, Plasma Phys. **24**, 451 (1982).
[40]A. P. Misra and A. R. Chowdhury, Fiz. A-Zagreb **11**, 163 (2002).
[41]P. K. Shukla and A. P. Misra, Phys. Lett. A **376**, 2591 (2012).
[42]A. P. Misra, Phys. Plasmas **21**, 042306 (2014).
[43]M. Salimullah and F. Majid, Phys. Rev. A **25**, 555 (1982).
[44]E. J. Parkes, J. Phys. A: Math. Gen. **20**, 3653 (1987).
[45]M. K. Alam and A. R. Chowdhury, Aust. J. Phys. **53**, 289 (2000).
[46]A. P. Misra and C. Bhowmik, Phys. Plasmas **14**, 012309 (2007).
[47]R. Sabry, W. M. Moslem, and P. K. Shukla, Plasma Phys. Controlled Fusion **54**, 035010 (2012).
[48]F. Verheest and S. R. Pillay, Phys. Plasmas **15**, 013703 (2008).
[49]T. Taniuti, Suppl. Prog. Phys. **55**, 1 (1974).
[50]W. Horton and Y. H. Ichikawa, *Chaos and Structures in Nonlinear Plasmas* (World Scientific, 1996), p. 187.
[51]A. Davey and K. Stewartson, Proc. R. Soc. London, Ser. A **338**, 101 (1974).
[52]B. Ghosh and K. P. Das, Plasma Phys. Controlled Fusion **27**, 969 (1985).